Environ Geol (2007) 52:259–267
DOI 10.1007/s00254-006-0538-0

ORIGINAL ARTICLE

Patterns of halite (NaCl) crystallisation in building stone conditioned by laboratory heating regimes

Miguel Gomez-Heras · Rafael Fort

Received: 15 June 2006 / Accepted: 26 September 2006 / Published online: 18 October 2006

Abstract The crystallisation of soluble salts within the pores of the stone is widely recognised as a major mechanism causing the deterioration of the stone-built architectural heritage. Temperature, in turn, is one of the main controls on this process, including salt precipitation, the pressure of crystallisation and the thermal expansion of salts. Most laboratory experiments on decay generated by salts are just carried out with convective heating regimes, while in natural environments building stones can undergo radiative and convective heating regimes. The thermal response of stone to these different heating regimes is noticeably different and might influence the crystallisation patterns of a salt within a stone. The aim of this work is to raise awareness on the different patterns of crystallisation of NaCl within a porous stone tested with different heating regimes (convection and radiation) and the implications that this could have on the design of experimental modelling of natural weathering conditions in laboratory simulations. Results show that heating regime affects the sodium chloride distribution within a stone with high percentage of microporosity. In this case, radiation heating facilitates the generation of subefflorescences, while convection heating promotes efflorescences. This has a clear implication both on the stone decay in natural environments and on the methodologies for testing salt decay, as subefflorescences are more destructive than efflorescences. In this sense, the use of convective heating in laboratory experimentation might underestimate the potential damage that sodium chloride may generate. This counsels the use of radiation heating test methods in addition to convection for the laboratory study of salt crystallisation.

Keywords Stone weathering · Salt decay · Temperature · Ageing tests · Experimental designs

M. Gomez-Heras (✉)
School of Geography, Archaeology and Palaeoecology,
Queen's University Belfast, Belfast BT7 1NN, UK
e-mail: m.gomez@qub.ac.uk

R. Fort
Instituto de Geología Económica (CSIC-UCM),
Facultad CC, Geológicas UCM, 28040 Madrid, Spain

Introduction

Laboratory testing of building materials is one of the most common methodologies to understand the decay processes they experience in natural environments. However, laboratory tests can never exactly replicate the processes that occur in natural environments. Building materials placed in the nature or in a building are affected by numerous decay agents, which act synergistically and are influenced by feedback mechanisms. Nevertheless, any laboratory simulation or accelerated ageing test carried out either for industrial or scientific purposes should seek to maximise the replication of the environments in which the tested materials are found either naturally or in use. In terms of the temperature regimes employed and salts, laboratory tests should use realistic absolute temperatures instead of extreme conditions (McGreevy and Smith 1982). This could be extended to the need of using realistic heating regimes.

Heat is propagated in nature by means of conduction, convection and radiation. Any material placed in

a building is going to be heated by the action of the surrounding air (convection) and directly by the sun on its surface (radiation). This heat income will be transferred through the materials by means of conduction. There is a wide literature on the differences between convective and radiative heating regimes as well as on the extent of the influence that temperature exerts on building stones through so-called 'insolation weathering' (e.g. Griggs 1936; Smith 1977; Warke et al. 1996; Warke and Smith 1998; Halsey et al. 1998; Hall and André 2003; Gomez-Heras et al. 2006). In contrast, literature on the influence of different heating regimes on other decay processes, such as the salt crystallization, is relatively scarce.

The crystallization of soluble salts within porous stones has been widely accepted as one of the most crucial mechanisms causing the deterioration of built heritage (e.g. Schaffer 1932; Correns 1949; Winkler 1973; Scherer 1999; Steiger 2005) along with recognition that crystallization process is influenced by temperature.

The crystallization of a salt within the pores of a stone takes place when a saline phase reaches supersaturation and the thermodynamic characteristics of the system are adequate for the formation of nuclei from which crystals can grow. In this study, temperature has been chosen as the main environmental parameter controlled in the experiments, although this is not the only factor influencing the crystallisation of salts. The composition of the solutions, pore distribution or humidity among others also control this process. Nevertheless, the specific importance of temperature in the context of salt weathering is highlighted by the fact that the rate of thermal expansion of salts can be much greater than that for the host stone. For example, the volumetric expansion of NaCl from 20 to 100°C is 0.933%, which is 15 times higher than the average volumetric expansion of a limestone (0.064%) for the same interval (Skinner 1966) The influence of these stresses has been previously identified as a possible contributor to decay generated by salts (Cooke and Smalley 1968; Winkler 1973).

However, the determination of the temperature regimes in the context of a building to be applied in a laboratory simulation is not straightforward, as heating regimes across a building can be very complex, and will vary spatially and temporally at different scales. Depending on the building orientation, some facades can experience episodes of 'pure' convective heating (as in a continuously shadowed façade) while others can undergo daily cycles of radiative heating (due to insolation) or a higher frequency cycling due to periodic shadowing during the course of a day. All of this generates disparate heating responses in the stones (Gomez-Heras et al. 2006).

Radiation heating promotes faster heating rates than convective heating for the same ambient temperature regime. In a stone heated merely by convection, the loss of energy in the transfer from air to stone is higher than in a stone heated by radiation, as it comprises movement of the particles of the air mass. Therefore, radiation heating generates higher surface temperatures and more complex temperature distributions at the surface and within the stone (e.g. Peel 1974; Warke and Smith 1998; Gomez-Heras 2006), although precise rates of heating are controlled by a number of variables including inter-granular differences (Hall and André 2003; Gomez-Heras et al. 2006). In contrast, convective heating tends to mask differences in thermal properties between the stone types to heating (Warke and Smith 1998). This means that differences between stone types driven by their thermal properties may be lost under convective heating regimes.

Because of the widespread use of convective heating in laboratory weathering simulations, the complexity of the temperature regimes that insolation (i.e. radiative heating) generate in naturally exposed stone is also largely lost. This includes most, if not all standards and experimental methodologies for salt testing that are based in ovens with forced air circulation and convective sources of heating (e.g. ASTM 1964; RILEM 1980; CEN 1999; Houck and Scherer 2006).

It is expected, that these differences in heating regime will in turn influence the way in which salts will crystallize under radiative and convective heating regimes. The influence of salt loading in an insolation environment has been previously reported (Smith et al. 2005) as well as the implications of different heating rates on the salts' morphologies (Smith and McGreevy 1988; Rodriguez-Navarro and Doehne 1999) and the importance of heating and cooling patterns as the result of aspect and shading differences has been acknowledged (Smith 1977, 1978). There are, however, no previous studies that have investigated the influence of experimental insolation and convection heating regimes on crystallization processes at a microscopic scale and the implications that this may have for the interpretations of laboratory decay tests.

As a consequence, the aim of this preliminary study is to raise awareness of the importance of heating regimes in the laboratory experimental simulation of salt decay by exemplifying the morphological and distribution differences of NaCl crystallised within a specific porous bioclastic limestone, as the result of two different heating regimes.

Materials and methods

The study is designed to compare the morphologies of NaCl crystals within blocks of a biomicritic limestone, as a result of different experimental heating regimes (convective and radiative) in a climatic cabinet. The experiments used 10 cm cubes of a biomicritic limestone commercially known as *Bateig Azul*. This is quarried in the province of Alicante and is a common building material in several regions of central and eastern Spain (Fort et al. 2002) and in use it is subject to a range of salt decay mechanisms. It was selected also on the basis of its relatively low albedo that should enhance differences between the convective and radiative heating regimes.

The petrography of the stone was characterised by polarizing microscope and colour, porosity, ultrasound velocity parameters and hydric behaviour were determined. Colour was measured with a spectrophotometer (*MINOLTA CM-2002*) with D65 illuminant and 10° standard observer. L*, a* and b* according to CIELAB system (CIE 1986) and white and yellow indexes according to ASTM E313 standard (ASTM 2000) were measured. Porosity parameters were characterized with a Mercury Intrusion Porosimeter (*Micrometritics Autopore IV*). *p*-waves ultrasound velocity (Vp) and anisotropy index (I_A) were measured with an ultrasonic pulse velocity meter (*PUNDIT, CNS*). The anisotropy index (I_A) was calculated as:

$$I_A = 100 \cdot \left(1 - \frac{2V_1}{V_2 + V_3}\right) \quad (1)$$

where V_1, V_2 and V_3 are the *p*-waves ultrasound velocities for each axis, being V_1 the lowest velocity. RILEM (1980) guidelines were used for hydric behaviour tests.

Heating experiments were conducted via one surface of rock cubes placed vertically within a climatic cabinet and exposed to either radiative or convective heating. The blocks were insulated on all other sides by a casing of expanded polystyrene of 0.5 cm thickness. The heated surface was selected to be perpendicular to any possible lamination in the stone. The calculation of the anisotropy index (I_A) of the material showed directionality, which was not macroscopically noticeable. Therefore, the surface exposed was selected to be perpendicular to the direction with lower Vp (V_1).

Stone blocks were dried in an oven until constant weight before the experiments began. Once dried, the blocks were immersed, without the polystyrene case, in a saturated NaCl solution for 48 h. Although total immersion does not replicate mechanisms such as capillary rise, whose importance in the context of a building can be high (Benavente et al. 2001), this method was selected as it is frequently used for laboratory salt testing (e.g. Goudie 1993; Goudie and Viles 1995). Single immersion was also preferred as it facilitated the comparison of the different tests. Immersion time was set to 48 h following the RILEM guidelines for saturation tests.

Sodium Chloride was selected, as it is a salt commonly found in buildings (Winkler 1973; Cooke 1994; Goudie and Viles 1997; Gomez-Heras et al. 2004) and frequently used in accelerated decay tests (e.g. Goudie 1974; Sperling and Cooke 1985; Grossi and Esbert 1994; Goudie and Viles 1997; Benavente 2003). In addition, sodium chloride does not present phase transitions that could complicate the interpretation of results, as opposed to other salts used in accelerated decay tests, such as sodium sulphate, that has a more complex system with phase transitions between thenardite and mirabillite.

Two experimental cabinets with a similar internal volume of 60 dm^3 were used. The cabinet used for convection tests was a *Memmert 400* with steady thermostat to which an external temperature programmer was attached. The heating in this cabinet was attained through forced air convection by means of a shielded fan that prevented direct blowing of air across the blocks. Radiation tests were carried out in an automatic cabinet designed specifically to carry out insolation tests through heating with infrared lamps without forced air circulation (Gomez-Heras and Fort 2002; Gomez-Heras 2006). In both cases, the cabinets were programmed with the same 4 h temperature cycle based on the average summer temperatures for the period 1993–1996 recorded at a climatic station at the Royal Palace of Madrid (Lopez de Azcona et al. 1996). The air temperature during the cycle oscillated between 23 and 37°C with an initial 30 min constant-speed heating ramp and 3.5 h of unforced cooling.

The relative humidity within the cabinets was set at 5%. This value, which could be considered unusually low in the context of buildings in temperate climates, was selected to minimize any effect that humidity might have in the crystallisation process and to isolate, as much as possible, the effects of heating regimes. To maintain the humidity, 100 g of silica gel with blue colour indicator was placed in each cabinet. The silica gel was periodically renewed during the experiments as required.

Changes in the specimens were visually controlled during the experiment with naked eye and under low magnification (10×). Weight loss through the drying of the samples was also controlled throughout the

experiments. Each experiment was stopped when the weight loss between successive cycles was less than 0.1‰ (around 565 cycles, depending on the specific experiment). The weights of the blocks were measured in external scales towards the end of the cycles when the sample temperature approximated to room temperature. In order to homogenize the weight loss figures for comparison, water saturation (S_w) percentage over total saturation was used instead of the absolute weights:

$$S_w = \frac{W - W_0}{W_S - W_0} \cdot 100 \quad (2)$$

where W_0 is the dry sample weight, W_S is the saturated (48 h) sample weight and W the weight of the sample at each stage of the experiment.

At the end of each test, the polystyrene case was removed and stone chips were removed for examination by scanning electron microscopy (SEM) from the heated surface and interior of the block. Samples were obtained from the blocks by successively splitting them using mechanical jaws. In this way, it was possible to obtain a series of stone 'chips' along a depth profile below the exposed surface. These samples were gold sputtered to be observed in a Jeol JSM 6400 Microscope in secondary electrons (SE-SEM) and backscattered electrons modes (BE-SEM).

Results

The *Bateig Azul* stone is a terrigenous-rich biomicrite (Fig. 1) with foraminifera, bryozoans and gastropods as the main bioclasts and quartz as main terrigenous clasts. Echinoderm spines and plates and calcareous red algae are also present, as well as feldspar and rock fragments (mainly dolomite and metamorphic rocks). The stone presents a matrix of micritic calcite together with siliceous cementation and drusy calcitic cement rims. The occurrence of glauconite as an accessory authigenic mineral is noticeable and is one of the causes of the bluish colour of the stone. Table 1 shows the average petrophysical parameters measured for this material.

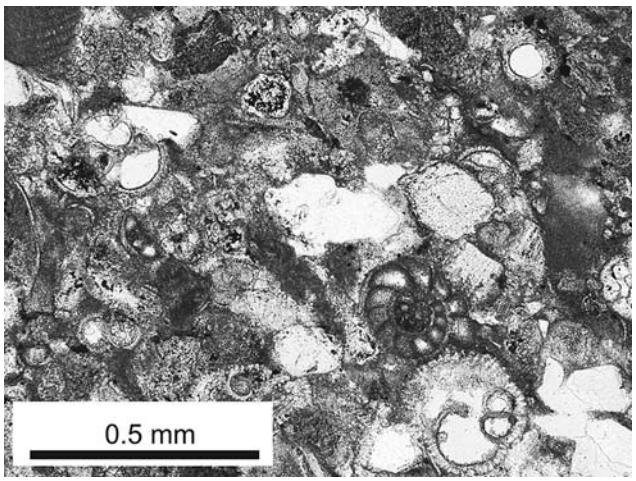

Fig. 1 Photomicrography of *Bateig Azul* with parallel polaroids

Figure 2 shows the evaporation of the solutions, expressed as the percentage of total water saturation for radiative and convective heating tests. These graphs show the evaporation rate. The inflexion point in the convection is much shorter (18 cycles; 72 h) than in the radiation tests (around 100 cycles; 400 h). For the first cycles (before the inflexion time of the convection test), the evaporation rate is lower under radiative heating than under convective heating. From this inflexion point onwards, the evaporation rate is lower under convective than radiative heating. The samples heated through convection reach a constant rate of weight loss before those heated by radiation.

Optical inspection of the samples showed that the main surface changes occurred after the first cycles. Samples heated only by convection showed evident NaCl efflorescences covering about one half of the surface, while samples heated by radiation showed little if any efflorescence—at most 1% of the surface. In this case, the efflorescences were formed due to nucleation on a mark produced during the handling of the sample. After cycle 18, surface changes were slight and there was no increase of the areas affected by efflorescence. The only noticeable change is a thickening of the NaCl cover in the samples heated by convection, and an increase in surface roughness on the samples heated by radiation.

After removal of the polystyrene case, different depth profiles were observed for the case of convection and radiation heating (Fig. 3). In both cases, the areas of the sample furthest from the heated surface displayed acicular radial NaCl crystals concentrated around a limited number of nuclei, while the areas closest to the heated surface displayed a more homogeneous pattern of salt distribution without fibrous crystals. In the samples heated by convection (Fig. 3a), the salt is distributed homogeneously only in the first 36 ± 7 mm; below this, NaCl shows fibrous morphologies.

The samples heated by radiation (Fig. 3b) show a layer of crystals of NaCl located within the first millimeter from the heated surface of the stone, generating an incipient spalling of the surface. Deeper in the

Table 1 Petrophysical parameters of the stone *Bateig Azul*

L	74.7 ± 0.9
a*	–0.7 ± 0.1
b*	5.5 ± 0.3
Whiteness index	28.6 ± 2.0
Yellowness index	10.1 ± 0.5
Water saturation wt (%)	5.48 ± 0.08
Porosity accessible to water (%)	12.60 ± 0.10
Compactness	0.87
Porosity accessible to mercury	14.4
Microporosity (< 5 μm) (% of total pores)	95.4
Bulk density (g/cm^3)	2.27
Apparent density (g/cm^3)	2.66
Specific surface (m^2/g)	5.53
Pore size median (μm)	0.14
Pore size mean (μm)	0.05
Ultrasound velocity Vp (m/s)	3,770 ± 30
Anisotropy index	5.92

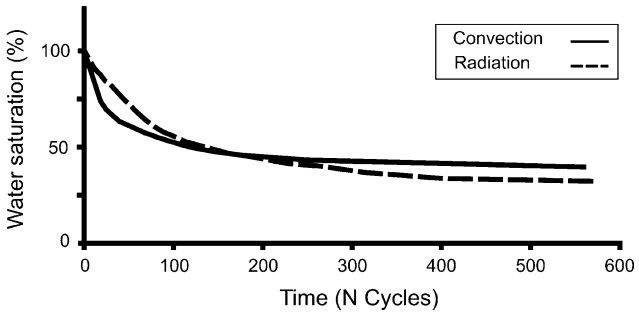

Fig. 2 Evaporation curves representative of tests carried out with convective (*solid line*) and radiative (*dashed line*) heating

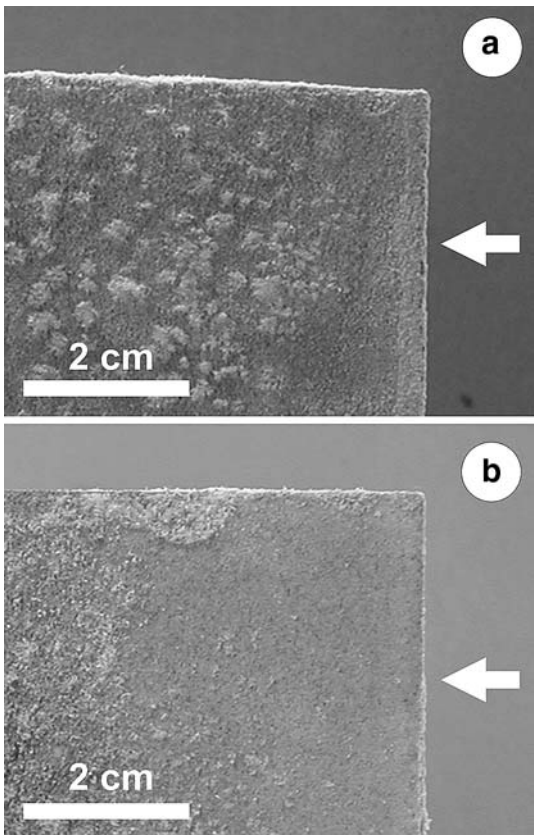

Fig. 3 Stone profiles of samples tested with convective (**a**) and radiative (**b**) heating. The *arrows* indicate the face that was exposed to heating

profile, an approximately 2.5 cm thick layer displays a homogeneous salt distribution without fibrous crystals. The first acicular crystals of NaCl begin to appear in the zone between 2.5 to 3.5 cm depth. Deeper than 3.5 cm, the predominant features are acicular radial NaCl crystals with a similar morphology to that displayed in the deepest areas of the samples heated by convection but with more nuclei.

Observations by SEM (Fig. 4) reveal noticeable morphological differences between the NaCl crystals formed under convection (Fig. 4a, c) and radiation (Fig. 4b, d). Under convection, NaCl appears as an efflorescence with an average thickness of c. 100 μm. Two main morphologies are observed: Firstly, homometric crystals placed in contact with the stone surface (Fig. 4a, bottom) or nucleated over other crystals in the external parts of the efflorescence. Secondly, the most abundant acicular crystal that display longitudinal fluting and are often curved (Fig. 4a, top). The external surface of these crystals presents an irregular morphology (Fig. 4c).

The NaCl crystals formed in the samples heated by radiation appear as subefflorescences at around 100 μm depth from the heated surface. The crystals form columns perpendicular to the heated surface (Fig. 4b) creating a salt layer of up to 300 μm in thickness. These crystals display oscillatory zoning parallel to the heated surface, as seen by means of BSE-SEM (Fig. 5). Each zone could be related to a pulse of growth of 23 ± 5 μm average thickness. The crystals nucleated within the pores created an interstitial layer that pushed away the stone surface. Some stone fragments are found included within the crystals in this interstitial layer.

Discussion

A qualitative model of the distribution of the NaCl within the stone regimes can be established for the experimental convective and radiative heating from the observations carried out (Fig. 6). The maximum occurrence of NaCl is at the surface of the material in the samples heated by convection. The abundance of NaCl crystals decreases rapidly towards the interior of the stone. The NaCl concentrates at a depth of around 100 μm in the samples heated with radiation to

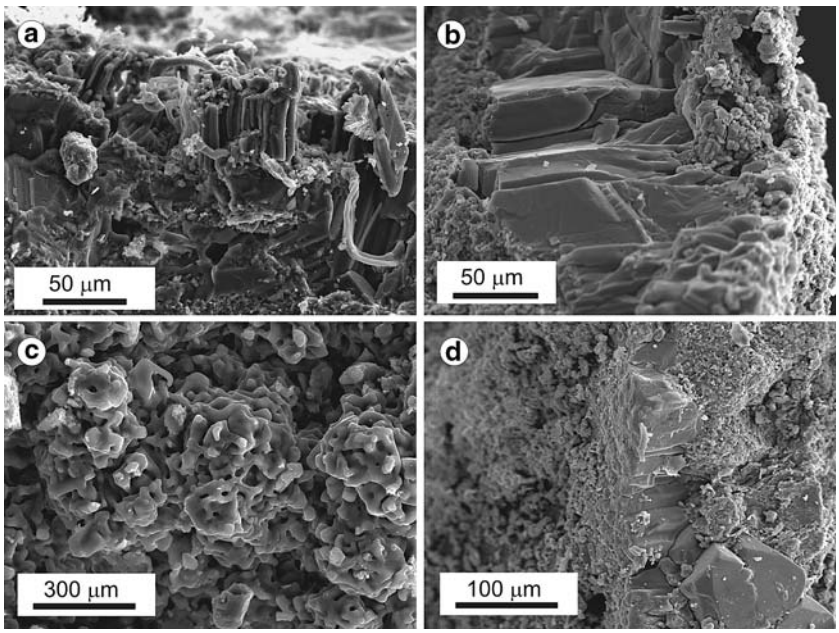

Fig. 4 SEM-SE images of NaCl crystallised after convective (**a**, **c**) and radiative (**b**, **d**) heating. They show the tendency of NaCl to form efflorescences after convective heating and subefflorescences after radiative heating

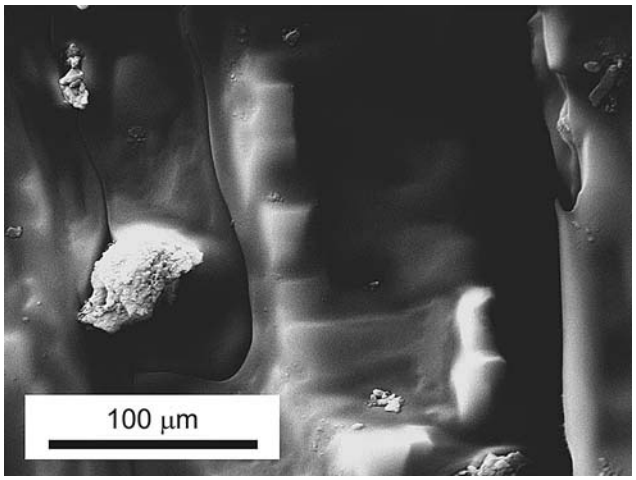

Fig. 5 SEM-BSE image of a NaCl crystal showing oscillatory zoning due to cyclic growing episodes

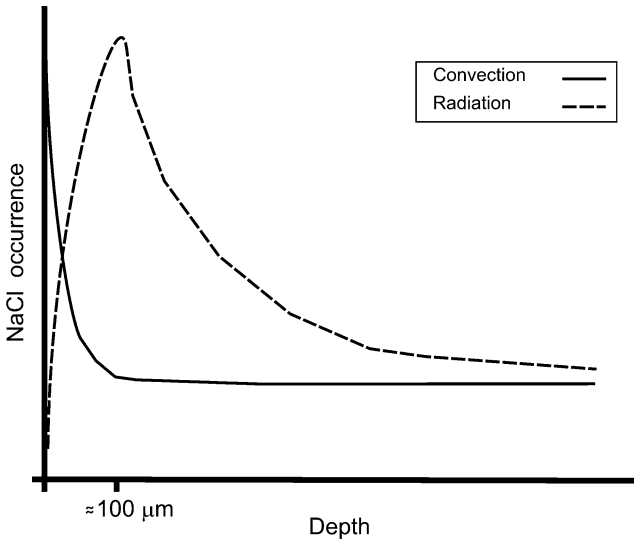

Fig. 6 Schematic non-quantitative model of bulk distribution of NaCl crystals for a stone heated with convective and radiative heating

decrease progressively towards the deeper areas of the stone.

The different mechanisms of evaporation and temperature profiles associated to the different heating regimes condition the dissimilar distributions and morphologies of the NaCl in the samples studied. The air movement and mass transfer generated under convective heating are not as crucial in promoting evaporation under radiative heating. The heating—cooling cycles through convection barely affect the first few millimetres of stone (Gomez-Heras 2006) while the cyclic heating generated by radiation generates higher surface temperatures and complex temperature distributions that affect to a noticeable thickness of stone (Peel 1974; Warke and Smith 1998; Gomez-Heras et al. 2006).

The final distribution and morphologies of NaCl are strongly conditioned by the behaviour of the solution in the first cycles as, once the first halite crystals appear, continued growth requires less energy than the initiation of new crystals. Moisture loss was channelled predominantly through the exposed heated surface by virtue of the polystyrene jacket and the solution progresses from the interior of the material to the surface by capillarity due to the loss of moisture at the surface.

Air circulation is an important control on evaporation in the case of the convective heating. The solution evaporates more rapidly in the case of convective heating than in the radiative heating due to the air movement at the stone's surface. This is reflected in the initial greater rate of moisture loss in the convection evaporation curves (Fig. 2). As NaCl crystallizes at and near the surface, it could act as a seal and slow down the evaporation process, as suggested by Smith et al. (2005).

In addition, the microporosity (pore size < 5 μm) of this material is high (95.4% of the total porosity). The evaporation is hindered in these stones in comparison to stones with greater pore size, as the evaporation of a saline solution is disfavoured in general (Benavente 2003).

As mentioned before, for the same regime of ambient temperatures, the rate of surface temperature increase is less under convective heating than under radiative heating, as the loss of energy in the heat transfer from the air to the stone is higher in convection than in radiation. In addition, due to the cyclic increase and decrease of ambient temperature, stone keeps a temperature lower than the ambient in most of the cycle (Warke and Smith 1998; Gomez-Heras 2006). Evaporation from the external surface of the stone will therefore be the main mechanism by which the solution attains the necessary level of supersaturation for the crystals to form. This conditions the nucleation of the halite crystals in the external surface of the material and therefore the formation of efflorescence. The observation of the NaCl distribution profile confirms that high supersaturations are only attained in the first half centimetre (high number of crystals, reflecting a high number of initial nuclei, and acicular crystallization patterns indicating fast growth). In the rest of the material, the signs of high supersaturation are dramatically lower below the immediate subsurface zone.

The temperature increase is more intense and faster in the radiative heating regime than in the convective heating regime for the same ambient temperatures. The stone surface attains temperatures up to 46.7°C for dry *Bateig* subjected to the same experimental conditions (Gomez-Heras 2006) and the air circulation on the surface is less relevant than in the case of convective heating. Rapid heating of the surface favours faster drying of the near surface zone than the actual ability of the solution to move upwards by capillary rise from the interior of the stone to the surface, and an air-solution-pore interface is formed in the interior of the stone. The high microporosity of this stone also contributes to this process. The stone dries in this case more due to water vapour transfer rather than mass transfer (as it was the case in the convective heating). The initial slower evaporation rate and the overheated surface create the thermodinamycal conditions favourable for the nucleation of halite crystals in a subsurface plane. First halite crystals are formed within the pores instead of at the surface and, once these first crystals have been nucleated, the solution will tend to feed the growth of the subefflorescences instead of forming new crystals on the external surface. The subefflorescences display sub-euhedral morphologies that suggest 3D growth mechanisms (Sunagawa 1981) and therefore moderate supersaturations of the solution could be inferred. The salts' distribution profile show that the area in which moderate supersaturations can be inferred is thicker than in the samples heated through convection.

Conclusions

The results of these tests show that the experimental heating regime can influence the dynamics of salt crystallization within the stone in addition to other factors, such as, for example, porosity. In the specific case of this experimental design, radiative heating facilitates the formation of subefflorescence of sodium chloride, while efflorescence is formed with convective heating for the same ambient temperature cycles. This is mainly because radiation heats faster than convection.

This raises awareness on the need of exploring the impact of the differences between convective and radiative heating regimes on the design of laboratory salt decay tests. These tests generally use convective sources of heating and discard radiation to heat the samples. In this specific case, the use of forced air convection in the experimental design could signify the underestimation of the effects of NaCl crystallisation within a porous stone in terms of disruption of its surface.

This is exemplified in these experiments, in which NaCl subefflorescences generated under radiation produce a partial disruption of the stone surface (which could evolve into micro-spalling), while the efflorescences formed with convective heating did not affect the structure of the material. The disruption generated under radiation is a sum of the stress generated within the pores by the crystallizing NaCl and the stress generated by the difference of thermal expansion between NaCl and limestone, which is enhanced by the higher temperatures attained within the stone under radiation.

The extrapolation of these results to the decay in natural environments can be linked to the relation that

some authors establish between slow heating rates and features, such as scaling and granular disaggregation, as opposed to rapid heating rates, which would favour spalling (Smith et al. 1987; Smith and McGreevy 1988). These experiments show that radiation, which involves rapid heating, facilitates the formation of a continuous layer of subefflorescences. As a result, the stone surface is displaced and an incipient 'micro-spalling' is generated. On the contrary, only individual grains are mechanically affected by efflorescences generated under convection.

The different results obtained from radiative and convective heating encourage the consideration of using both types in the design of laboratory simulated salt decay tests. This would provide a truer reflection of the different 'heating scenarios' a stone block can undergo in natural environments. Convection and radiation combine on buildings even at block and grain scales as, for example, when a stone block in a corner position receives sunlight only on one side. As a consequence, it is likely that two very disparate salt crystallisation patterns will be generated.

This study highlights the importance of heating regimes and temperature distributions within the stone as influencing factors for the patterns of crystallisation of a salt within a porous stone. Nevertheless, the crystallisation of salts in porous stones is a complex process which is not only influenced by temperature. As in this example, microporosity can enhance the differences attained under both regimes. Further research should focus on the interaction of the different heating regimes with other parameters, such as variations of relative humidity, pore distribution or composition of solutions.

Acknowledgments This work was fully carried out at the *Instituto de Geología Económica (CSIC-UCM)*. Support of the project MATERNAS_CM 0505/MAT/0094 (Madrid's Regional Government, Spain) is gratefully acknowledged. We wish to thank Bateig Piedra Natural S.A. for supplying samples, Dr. M. Alvarez de Buergo for technical assistance and Dr. D. Benavente and Prof. B.J. Smith for their comments on the manuscript. We would also like to express our gratitude to Dr. Doerhoefer and another, anonymous, reviewer whose comments have been of great help for the improvement of this paper.

References

ASTM (1964) C218 Method of test for combined effect of temperature cycles and weak salt solution on natural building stone. ASTM, West Conshohocken, Pennsylvania

ASTM (2000) E313–00 Standard practice for calculating yellowness and whiteness indices from instrumentally measure color coordinates. ASTM, West Conshohocken, Pennsylvania

Benavente D (2003) Modelización y estimación de la durabilidad de materiales pétreos porosos frente a la cristalización de sales. Biblioteca Virtual Miguel de Cervantes, http://www.cervantesvirtual.com/FichaObra.html?Ref = 12011 Last access: 15/06/2006

Benavente D, García del Cura MA, Bernabéu A, Ordoñez S (2001) Quantification of salt weathering in porous stones using an experimental continuous partial immersion method. Eng Geol 59:313–325

CEN, (1999) EN 12370. Natural stone test methods—determination of resistance to salt crystallisation. Bruxelles

Cooke RU (1994) Salt weathering and the urban water table in deserts. In: Robinson DA, Williams RBG (eds) Rock weathering and landform evolution. Wiley, Chichester, pp193–205

Cooke RU, Smalley IJ (1968) Salt weathering in deserts. Nature 220:1226–1227

Correns CW (1949) Growth and dissolution of crystals under linear pressure. Disc Faraday Soc 5:267–271

Fort R, Bernabeu A, García del Cura MA, López de Azcona MC, Ordoñez S, Mingarro F (2002) Novelda stone: widely used within the Spanish architectural heritage. Materiales de Construcción 52(266):19–32

Gomez-Heras M (2006) Procesos y formas de deterioro térmico en piedra natural del patrimonio arquitectónico. Madrid: UCM, Servicio de Publicaciones. http://www.ucm.es/BUCM/tesis/geo/ucm-t28551.pdf Last access 15/06/06

Gomez-Heras M and Fort R (2002) Cámara automática para envejecimiento de materiales de construcción por insolación. In. Spanish patent, app n° 200201376: CSIC, p 19

Gomez-Heras M, Benavente D, Alvarez de Buergo M, Fort R (2004) Soluble salt minerals from pigeon droppings as potential contributors to the decay of stone based cultural heritage. Eur J Mineral 16:505–509

Gomez-Heras M, Smith BJ, Fort R (2006) Surface temperature differences between minerals in crystalline rocks: implications for granular disaggregation of granites through thermal fatigue. Geomorphology 78(3–4):236–249

Gomez-Heras M, Smith BJ, and Fort R (2006) Influence of surface heterogeneities of building granite on its thermal microenvironment and its potential for the generation of thermoclasty. Build Environ (in press)

Goudie AS (1974) Further experimental investigation of rock weathering by salt and other mechanical processes. Zeitschr. Geomorphologie N. F. Suppl. Bd. 21:1–12

Goudie AS (1993) Salt weathering simulation using a single-immersion technique. Earth Surf Process Landf 18:369–376

Goudie AS, Viles HA (1995) The nature and pattern of debris liberation by salt weathering: a laboratory study. Earth Surf Process Landf 20:437–449

Goudie AS, Viles HA (1997) Salt weathering hazards. Wiley, Chichester

Griggs DT (1936) The factor of fatigue in rock exfoliation. J Geol 44:783–796

Grossi C.M, Esbert RM (1994) Las sales solubles en el deterioro de rocas monumentales; revisión bibliográfica. Materiales de Construcción. 44:15–30

Hall K, Andre M-F (2003) Rock thermal data at the grain scale: applicability to granular disintegration in cold environments. Earth Surf Process Landf 28:823–836

Halsey DP, Mitchell DJ, Dews SJ (1998) Influence of climatically induced cycles in physical weathering. Quart J Eng Geol 31:359–367

Houck J, Scherer GW (2006) Controlling stress from salt crystallization. In: Kourkoulis SK (ed) Fracture and failure of natural building stones. Proceedings of the international

symposium on fracture and failure of natural building stones within the frame of the 16th European conference on fracture, Alexandroupolis, Hellas, July 2006. Springer, Dordrecht, The Netherlands

López de Azcona MC, Mingarro F, Fort R (1996) Estudio Medioambiental en el Palacio Real de Madrid. Geogaceta 20:1155–1158

McGreevy JP, Smith BJ (1982) Salt weathering in hot deserts: observations on the design of simulation experiments. Geografiska Annaler 65A:161–170

Peel RF (1974) Insolation weathering: some measurements of diurnal temperature changes in exposed rocks in the Tibesti region, central Sahara. Zeitschrift für Geomorphologie N. F. Suppl. Bd. 21:19–28

RILEM (1980) Recommended tests to measure the deterioration of stone and to assess the effectiveness of treatment methods (V-1a, V-1b, V-2). Mater Struct 75:175–253

Rodriguez-Navarro C, Doehne E (1999) Salt weathering: influence of evaporation rate, supersaturation and crystallization pattern. Earth Surf Process Landf 24:191–269

Schaffer RJ (1932) The weathering of natural building stones. Building research establishment, Watford

Scherer GW (1999) Crystallisation in pores. Cement Concrete Res 29:1347–1358

Skinner BJ (1966) Thermal expansion. In: Clark SP (ed) Handbook of physical constants.. Geological Society of America Memoir 97

Smith BJ (1977) Rock temperature measurements from the northwest Sahara and their implications for rock weathering. CATENA 4(1–2):41–63

Smith BJ (1978) Aspect related variations in slope angle near Béni Abés.Western Algeria, Geografiska Annaler 60A:175–180

Smith BJ, McGreevy JP (1988) Contour scaling of a sandstone by salt weathering under simulated hot desert conditions.Earth Surf Process Landf 13:697–706

Smith BJ, McGreevy JP, Whalley WB (1987) The production of silt-size quartz by experimental salt weathering of a sandstone. J Arid Environ 12:199–214

Smith BJ, Warke PA, McGreevy JP, Kane HL (2005) Salt-weathering simulations under hot desert conditions: agents of enlightenment or perpetuators of preconceptions? Geomorphology 67(1–2):211–227

Sperling CHB, Cooke RU (1985) Laboratory simulation of rock weathering by salt crystallization and hydration processes in hot, arid environments. Earth Surf Process Landf 10(6):541–555

Steiger M (2005) Crystal growth in porous materials–I: the crystallization pressure of large crystals. J Cryst Growth 282:455–469

Sunagawa I (1981) Characteristics of crystal growth in nature as seen from the morphology of mineral crystals. Bull de Minéralogie 104:81–87

Warke PA, Smith BJ (1998) Effects of direct and indirect heating on the validity of rock weathering simulation studies and durability tests. Geomorphology 22(3–4):347–357

Warke PA, Smith BJ, Magee RW (1996) Thermal response characteristics of stone: implications for weathering of soiled surfaces in urban environments. Earth Surf Process Landf 21:295–306

Winkler EM (1973) Stone: properties, durability in man's environment. Springer, Berlin Heidelberg New York, 230 pp